Journal of the Serbian Chemical Society
JSCS-info@shd.org.rs • www.shd.org.rs/JSCS

ACCEPTED MANUSCRIPT

Journal of the Serbian Chemical Society
JSCS-info@shd.org.rs • www.shd.org.rs/JSCS
*J. Serb. Chem. Soc.***00(0)** 1-19 (2024)
JSCS–13000
Original scientific paper
Published DD MM, 2024

Thermal, morphological and surface properties of composite materials with perlite reinforcement

CEYDA BİLGİÇ[1]*, NAİLE KARAKEHYA[2], ADAM VOELKEL[3]

[1]Department of Chemical Engineering, Faculty of Engineering and Architecture, Eskişehir Osmangazi University, Eskişehir, Türkiye, [2]Department of Environmental Protection Technologies, Eskişehir Vocational School, Eskişehir Osmangazi University, Eskişehir, Türkiye, and [3]Poznan University of Technology, Institute of Chemical Technology and Engineering, Poznań, Poland.

(Received 8 August; revised 6 October; accepted 10 November 2024)

Abstract: This paper deals with the preparation and characterization of perlite/polyvinyl alcohol, perlite/polyvinylpyrrolidone, perlite/polymethyl methacrylate, and perlite/polystyrene composites. Polymer composites were prepared by solvent casting technique with 5 wt. % of perlite filler. Perlite is a filler with unique properties, such as low density and thermal conductivity, thus the development of Polymer-Perlite composites may be interesting for producing lighter packaging with thermal insulation capability. The perlite/polymer nanocomposites were characterized using X-ray diffraction (XRD) analysis, thermogravimetric analysis (TGA), Fourier-transform infrared spectroscopy (FTIR), inverse gas chromatography (IGC), field emission scanning electron microscopy (FE-SEM) and transmission electron microscopy (TEM). TGA measurements showed remarkable increases in the thermal stability of the polystyrene by the perlite loading as compared to the matrix. The FE-SEM image of the cryomilled sample shows that the perlite particles were embedded within a polystyrene matrix. This finding is consistent with the work of adhesion data obtained by IGC.

Keywords: polyvinyl alcohol; polyvinylpyrrolidone; polymethyl methacrylate; polystyrene; inverse gas chromatography.

INTRODUCTION

Perlite is a naturally occurring granular material and is mainly composed of SiO_2 and Al_2O_3. The lightweight, low cost, and low thermal conductivity properties of perlite can enable it to be used as a filler in polymers. The incorporation of perlite into the polymer matrix can improve the mechanical, thermal, and barrier properties of the final product. Sahraeian *et al.*[1] have studied the rheological,

* Corresponding author. E-mail: cbilgic@ogu.edu.tr
https://doi.org/10.2298/JSC240808093B

thermal, and dynamic mechanical properties of low-density polyethylene/perlite nanocomposites. The results revealed that the dynamic mechanical properties and thermal stabilities of nanocomposites were improved by the addition of surface-treated nano-perlite. In another study, de Oliveira *et al.*[2] investigated the effect of expanded perlite content on the morphological, mechanical, thermal, and rheological properties of polystyrene/expanded perlite composites. Doğan *et al.*[3] prepared chitosan/perlite nanocomposites using the solvent casting method. Perlite was dispersed homogeneously in the chitosan matrix. The thermal stability of chitosan after perlite incorporation was improved. They have also found that the hydrophilic properties of nanocomposites increased with increasing perlite content. Tian and Tagaya,[4] focused on the preparation of poly (vinyl alcohol) (PVA)/perlite nanocomposites. They have found that the heat resistance of PVA was enhanced by perlite addition. Raji *et al.*[5], utilized two perlite structures (raw or expanded) as filler in polypropylene-based composites. They have found that better dispersion and interfacial adhesion of the raw perlite in the polypropylene matrix was achieved compared to the expanded perlite. As mentioned above, there have been numerous studies to investigate perlite-filled polymer composites. However, to the best of our knowledge, perlite-reinforced PVP-based composites have not been found in the literature.

Inverse gas chromatography (IGC) is a versatile, powerful, sensitive and relatively fast technique for characterizing the physicochemical properties of materials. Due to its applicability in determining surface properties of solids in any form such as films, fibers and powders of both crystalline and amorphous structures, IGC became a popular technique for surface characterization, used extensively soon after its development. The properties that can be determined using the IGC technique include enthalpy and entropy of sorption, surface energy (dispersive and specific components), work of adhesion/co-adhesion, miscibility and solubility parameters, surface heterogeneity, glass transition temperature, and Lewis acid–base parameters. One of the greatest advantages of this method is that no special sample preparation is required. In fact, IGC requires the minimum sample preparation when compared to other surface energy analyzing techniques. Therefore, various forms of solids and even semi-solids can be characterized quickly and efficiently. The knowledge of surface properties of solids has great technological importance for all interfacial phenomena, as it is a very useful parameter in studies of adsorption and wettability processes.[6-10]

Polymer composites have been widely used in various areas of transportation vehicles, construction materials, packaging industry, electronics and sporting goods and consumer products. The synthesis and development of polymer/silicate composites have attracted considerable attention from both basic research and commercial applications, as they often exhibit remarkable improvements in the mechanical properties, thermal stability, gas barrier properties, enhanced ionic

conductivity, reduced flammability and biodegradation, etc., as compared with the pure polymers or conventional micro- and macro-composites. These improvements in the properties are the result of the nanometer scale dispersion of silicate in the polymer matrix. The dispersion of clay layers in a monomer or polymer matrix can result in the formation of three types of composite materials. The first type is a intercalated, that can be formed if the interlayer distance increases but the layer morphology remains unchanged, an intercalated nanocomposite structure is obtained. The other type is intercalated-and-flocculated conceptually the same as intercalated nanocomposites. The last type is the exfoliated structure, which can only be obtained if the silicate layers totally disperse in the polymer matrix. Exfoliated polymer–silicate nanocomposites are especially desirable for improved properties because of the homogeneous dispersion of clay and huge interfacial area between polymer and silicate.[11-13]

Polymers and polymer composites are used in a wide range of areas in daily life due to their superior properties such as being highly durable, lightweight, hygienic and flexible to process. Most polymer products do not decompose in nature and cause serious environmental pollution.

Due to the negative effects of today's traditional polymers on human and environmental health and their centuries-long recycling, biodegradable polymers that can decompose in nature are increasing their importance day by day. The features that make biopolymers superior to traditional polymers can be summarized as; easy decomposition, reducing dependence on fossil fuels, not leaving a toxic effect, being easier to recycle, requiring less energy in their production, being renewable and ecological. In this article; nanocomposite materials were prepared using

polystyrene and polymethyl methacrylate polymers, which are used extensively in industrial areas, and polyvinyl alcohol and polyvinyl pyrrolidone polymers, which have biodegradable (environmentally friendly) properties. The method of solvent casting used in the preparation of polymer nanocomposites is the most common method used in the preparation of homogeneously distributed nanocomposites. Thanks to the solvent casting method, it is easy to control the concentrations of polymer and inorganic components. Using this method, which does not require special equipment and has been widely preferred for years due to its easy applicability, homogeneously distributed silicate/polymer nanocomposites were obtained. Polymer nanocomposites containing 5% filler (perlite) by weight were prepared using four different polymer matrices by the solvent casting method. Thus, the functionality, flexibility, coatability, wetting and adhesion, thermal and mechanical strength performances of the materials were improved by ensuring homogeneous distribution (exfoliated) of the nanofillers in the polymer matrices. The characterization of the structural, morphological, thermal, surface and interface properties of the obtained nanocomposites was carried out using many

analysis techniques (FTIR, XRD, SEM, TEM, TGA and IGC). In addition, it was aimed that the obtained nanocomposites would be an alternative to traditional nanocomposites in industrial applications due to their properties such as being lightweight, having a low carbon footprint, and having high thermal and mechanical properties. Another aim of the study is to produce innovative polymer nanocomposites with superior properties compared to traditional nanocomposites, as well as making a difference in the literature in many ways.

In this study, we investigated the use of perlite as reinforcement in various polymer matrix composites. For this work, we selected PVA, PVP, PMMA, and PS. PVP and PVA are water-soluble, low cost and easily available synthetic polymers of great industrial importance. They have been commonly used in medical and pharmaceutical applications.[14] PMMA and PS are well-known and widely used thermoplastic polymers for several industrial applications. The effects of incorporating perlite into PVA, PVP, PMMA, and PS were investigated using FTIR, XRD, TGA, FE-SEM, and TEM. Furthermore, surface free energy (γ_S), Lewis acidic parameter (K_A), and Lewis basic parameter (K_B) of the examined solids and work of adhesion between perlite and polymers were determined by using IGC.

IGC Background

In the IGC study, the retention times of probes were measured at infinite dilution conditions, allowing us to determine the interactions between the probes and the solid where lateral probe–probe interactions are negligible.[15,16] The first value determined is the net retention volume (V_N) of the probes;[17]

$$V_N = F.J.(t_R - t_M).(T/T_A) \quad (1)$$

where F is the flow rate of the carrier gas, J is the compression correction factor, t_R is the probe retention time, t_M is the dead time which is determined with methane, T is the column temperature and T_A is the ambient temperature.

The surface free energy (γ_S) of a solid has two components, the dispersive component (γ_S^d) and the specific component (γ_S^{sp}). The dispersive component results from the relatively weak van der Waals dispersion forces (London forces, Debye forces, and Keesom forces) and the specific component includes all of the polar forces (dipole forces and acid-base forces).

$$\gamma_S = \gamma_S^d + \gamma_S^{sp} \quad (2)$$

In this study, γ_S^d values were calculated according to the Schultz-Lavielle method;[18]

$$R.T.ln(V_N) = 2.N.a.\sqrt{\gamma_S^d}.\sqrt{\gamma_L^d} + C \quad (3)$$

where R is the gas constant, N is Avogadro's number, a is the cross-sectional area of the probe, γ_L^d is the surface tension dispersive component of the probe and C is the constant.

The free energy of adsorption has dispersive and acid-base components. The specific component of the adsorption-free energy (ΔG^{sp}) is related to the electron donor/acceptor ability of the probe;[19]

$$\Delta G^{sp} = -R.T.ln\left(\frac{V_{N_{sp}}}{V_{N_{ref}}}\right) \quad (4)$$

Where $V_{N_{sp}}$ is the retention volume of a polar probe and $V_{N_{ref}}$ is the specific retention volume of n-alkanes with the same $a.\sqrt{\gamma_L^d}$ value as the polar probes. The specific component of the adsorption (ΔH^{sp}) was determined from the temperature dependency of ΔG^{sp};

$$\Delta G^{sp} = \Delta H^{sp} - T.\Delta S^{sp} \quad (5)$$

where is ΔS^{sp} the entropy of adsorption corresponding to the specific interactions.

Gutmann and van Oss concepts are very common approaches to determining the acid-base character of solid surfaces.[20] According to the Gutmann approach, specific interaction enthalpies between adsorbent and adsorbed correlate with acid-base properties.[21]

$$-\Delta H^{sp} = K_A.DN + K_D.AN^* \quad (6)$$

where K_A and K_D are the electron-accepting (acid) number and electron-donating (base) number of the examined solid surface, respectively. AN^* is the acceptor number and DN is the donor number of the polar probes.[22]

On the other hand, the work of adhesion between the perlite and the polymers was calculated according to the following equations;[6]

$$W_a^{tot} = W_a^d + W_a^{sp} \quad (7)$$

$$W_a^d = 2.\sqrt{\gamma_1^d.\gamma_2^d} \quad (8)$$

$$W_a^{sp} = 2.(\sqrt{\gamma_1^+.\gamma_2^-} + \sqrt{\gamma_1^-.\gamma_2^+}) \quad (9)$$

Where W_a^{tot}, W_a^d, and W_a^{sp} are the total work of adhesion, dispersive component, and specific component of work of adhesion, respectively. In Eq. (8), γ_1^d and γ_2^d are the dispersive components of the free surface energy of perlite and polymer, respectively. In Eq. (9), γ^+ and γ^- are the acidic and basic parameters of solids 1 (perlite) and 2 (polymer), respectively. For the calculation of γ^+ and γ^-, trichloromethane (TCM) and ethyl acetate (EA) were used[6].

$$\gamma^+ = \Delta G_{EA}^{sp}/(4.N^2.a_{EA}^2.\gamma_{EA}^-) \quad (10)$$

$$\gamma^- = \Delta G_{TCM}^{sp}/(4.N^2.a_{TCM}^2.\gamma_{TCM}^+) \quad (11)$$

The values of γ_{EA}^{-} and γ_{TCM}^{+} were taken as 6.2 mJ/m^2 and 1.5 mJ/m^2, respectively.[23]

EXPERIMENTAL

Materials

The crushed raw perlite sample was obtained from Cumaovası Perlite Processing Plants of Etibank (İzmir, Turkey). The chemical composition of Turkish perlite is reported earlier in literature and it consisted mainly of 71-75 % SiO_2, 12.5-18 % Al_2O_3, 2.9-4 % Na_2O, 4-5 % K_2O, 0.5-2 % CaO and 0.1-1.5 % Fe_2O_3.[24] The decantation and centrifugation process was used to remove dust and other water-soluble matter from perlite. About 50 grams of perlite was mixed with 1 L of distilled water in a beaker. This mixture was then covered and left for 2 days. Then, the top and middle part of the mixture was drawn with a pipette and the remaining sediment was removed from the process as waste. Centrifugation (about 20 min at 8,000 rpm) has been used to separate perlite from the suspension. The resulting perlite was diluted with 1 L of distilled water again. This process was repeated several times until there was no sediment visible on the bottom of the beaker. Subsequently, the residual perlite was dried for 24 h at 80 °C. Then it was milled into fine powder using a Retsch cryogenic grinder and sieved to obtain a particle size distribution between 60 and 100 µm. The specific surface area (by multipoint BET analysis) of purified perlite was 3.5 $m^2.g^{-1}$, perlite/PVA was 9.855 $m^2.g^{-1}$, perlite/PVP was 5.279 $m^2.g^{-1}$, perlite/PMMA was 8.025 $m^2.g^{-1}$ and perlite/PS was 11.48 $m^2.g^{-1}$ (Quantachrome, Autosorb-6). Therefore, the highest surface area belongs to the perlite/PS nanocomposite, which provides the highest performance properties. Poly(methyl methacrylate) (Mw~120,000), polystyrene (Mw~280,000), polyvinylpyrrolidone (Mw~1,300,000), poly(vinyl alcohol) (Mw~85,000-124,000) and all other chemicals were purchased from Sigma-Aldrich.

Preparation of nanocomposites

Four different kinds of composites, perlite/PVA, perlite/PVP, perlite/PMMA, and perlite/PS were prepared via the solvent casting technique. First, 0.5 g of perlite was added to 200 ml solvent and the mixture was stirred with magnetic stirring at 50 °C for 2 h. Then, 9.5 g of polymer was dissolved in 300 ml of the same solvent. The filler mixture was slowly added to the polymer solution. Polymer-filler mixture was stirred at 50 °C for 4 h. The mixture was submitted to sonication in an ice/water ultrasonic bath for 30 minutes at 35 kHz. At the end of the process, the dispersion was poured into glass Petri dishes and the solvent was evaporated at room temperature in a chemical hood. The solvent for perlite/PVA and perlite/PVP composites was distilled water while chloroform for perlite/PMMA and perlite/PS composites. Polymer films were ground to powder in a cryo-mill under constant cooling with liquid nitrogen (Retsch CryoMill, Germany) before the characterization step. The composite samples were named PVP-PER, PVA-PER, PS-PER and PMMA-PER. Each composite contained the 5 wt % of perlite.

Characterization techniques

The composite samples and perlite were sieved to pass a 60 µm for XRD and TEM analysis and the 150–200 µm sieve fraction was used for FE-SEM, TGA, and IGC analysis. The XRD analysis was carried out between 1 and 50° (2θ) at a scanning speed of 0.02° min^{-1} by a diffractometer (Rigaku Ultima-IV, Japan) with CuKα radiation (40kV/30mA). Thermogravimetric analysis (TGA) was conducted using a simultaneous thermal analyzer (Perkin Elmer STA 8000, USA) under a flowing N_2 atmosphere at a scan rate of 10 °C min^{-1} from 25 °C to 725 °C. FT-IR (Fourier transform infrared spectroscopy) analysis was performed

on Perkin Elmer Spectrum Two IR spectrometer (USA) using the KBr technique in the range 400–4000 cm^{-1} with a resolution of 1 cm^{-1}.

Inverse gas chromatography (IGC) measurements were carried out using a gas chromatograph (Agilent 7890A, USA), equipped with a flame ionization detector. A series of *n*-alkanes (*n*-heptane, *n*-octane, *n*-nonane, and *n*-decane) and polar solutes (tetrahydrofuran, diethyl ether, acetone, ethyl acetate, trichloromethane) were injected at infinite dilution conditions. The injection volume was 0.1 µL (liquid). Nitrogen was used as the carrier gas with a flow rate of 40 ml/min. Measurements were carried out at four different column temperatures (40, 50, 60, and 70 °C). The temperatures of the injector and detector were 150 °C and 200 °C, respectively. For each analysis, approximately 1 g of the examined material was packed into the stainless steel gas chromatography column (1.5 m long, 5.35 mm I.D.) closing both ends with glass wool. The columns were conditioned at 70 °C under the N_2 flow for 4 h. A non-adsorbing standard molecule (methane) was used to determine the dead time.

Detailed morphological characterization of the examined samples was performed by field emission scanning electron microscopy (FE-SEM, Regulus 8230, Hitachi, Japan) and transmission electron microscopy (TEM, HT7800, Hitachi, Japan). Before FE-SEM observation, samples were coated with a thin layer of gold using a sputter coater (EM ACE 600, Leica, Germany). TEM samples were prepared by placing a drop of a dilute suspension of nanocomposite powders on a carbon-coated copper TEM grid and allowing it to dry at room temperature.

RESULTS AND DISCUSSION

X-ray diffraction analysis

X-ray diffraction (XRD) analysis was used to reveal the structure of the polymers before and after the incorporation of perlite. As can be seen in Fig. 1, a broad peak appeared between 16 and 30° indicated that perlite was mainly amorphous.[25] PVA is known to be a crystalline polymer and pure PVA has three diffraction peaks at 2θ = 20°, 23° and 41°.[26] On the other hand, the XRD pattern of pure PVP showed two broad peaks centered at about 2θ = 12° and 21°, giving a sign that it is an amorphous polymer.[27] The pure PMMA sample exhibited three broad XRD peaks with their intensity decreasing systematically. These broad diffraction peaks approximately at about 2θ = 14°, 30° and 42° denoting the amorphous structure of the PMMA, and they have also been observed in other works.[28,29] PS exhibits two typical broad peaks at 2θ=11° and 19°. Similarly, the absence of sharp crystalline peaks indicates an amorphous structure in the XRD pattern of the pure PS.[30]

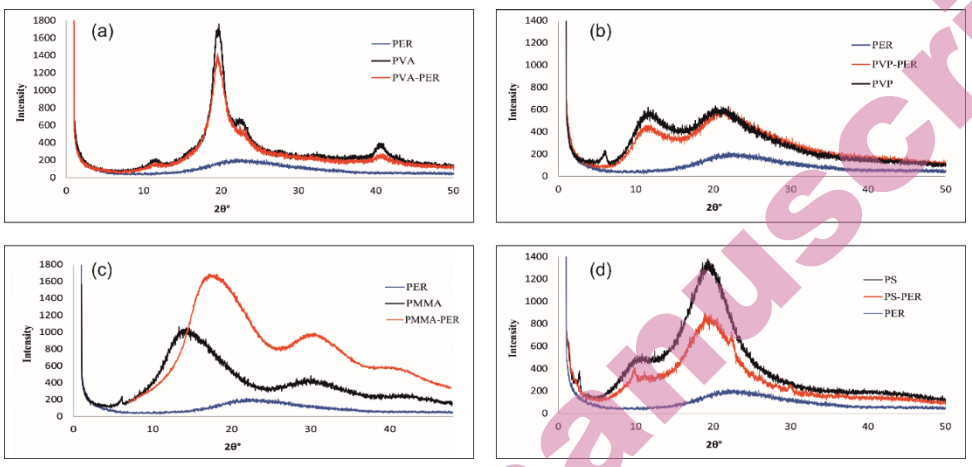

Fig. 1. X-ray diffraction patterns of perlite, neat polymers, and perlite/polymer composites.

Thermogravimetric analysis

TGA is a standard method to study the overall thermal properties of polymers, polymer blends, and polymer composites. The thermal behaviors of the perlite, neat polymers, and perlite/polymer composites are presented in Fig. 2. The results obtained from these curves are summarized in Table 1. The amount of char residue (percentages by weight at 600 °C), the temperatures of 5 % ($T_{0.05}$), and 50 % weight loss ($T_{0.5}$) are the main criteria indicating the thermal stability of the polymer composites. As shown in Figure 2, the thermal stability of perlite is very high and the char residue was determined as 98.5 % at 600 °C. It is worth mentioning that the initial drop at low temperatures (~50-150 °C) in the TGA graph of PVA and PVP indicates that the PVA and PVP contained physisorbed water.[31]

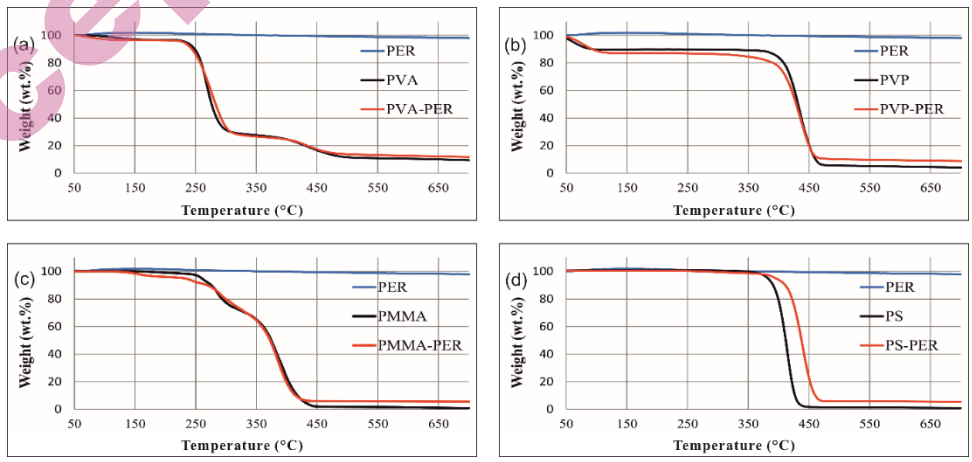

Fig. 2. TGA curves of perlite, neat polymers, and perlite/polymer composites.

TABLE I. Thermal stability of perlite, neat polymers, and perlite/polymer composites

Samples	$T_{0.05}$ (°C)	$T_{0.5}$ (°C)	Char at 600 °C (wt. %)
PVA	234	276	10.5
PVA-PER	229	283	12.6
PVP	62	432	4.8
PVP-PER	72	429	9.4
PMMA	260	374	1.4
PMMA-PER	231	373	5.7
PS	382	412	1.2
PS-PER	395	438	5.7

FTIR characterization

FTIR spectra of pure materials and the composites were presented in Fig. 3. The spectrum of the perlite can be identified with the following major peak assignments: Si–O rocking vibration (460 cm^{-1}), symmetric and asymmetric stretching vibration of Si–O–Si (790 cm^{-1} and 1060 cm^{-1}), stretching O–H vibrations which indicate the presence of isolated and surface Si-OH groups (broad band between 3190-3690 cm^{-1}).[32-34] There wasn't a notable discrepancy between the FTIR spectrum of the PVA including perlite and the spectrum of pure PVA.

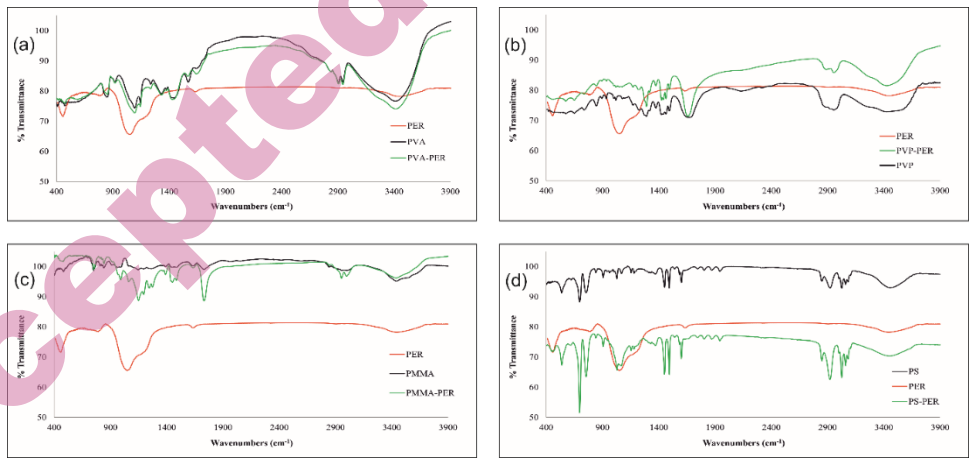

Fig. 3. FTIR curves of perlite, neat polymers and perlite/polymer composites.

Typical FTIR bands in PMMA are; 3000 and 2950 cm^{-1} C-H stretching vibrations of methyl group, 1730 cm^{-1} the C=O stretching vibrations of ester group, 1450 and 1300 cm^{-1} asymmetric and symmetric C-H deformation vibrations, 1165 cm^{-1} the stretching vibrations of ester group 990, 850 and 750 cm^{-1} C-H vibrations out of the ring.[35] Some differences were observed in the FTIR spectrum after the perlite addition into the PMMA matrix. The most important was the increasing intensity of the band at about 1730 cm^{-1} related to the C=O stretching vibrations

of ester group. It implies that there is an interaction of perlite and C=O of ester in PMMA via a coordination bond involving the hydrogen bond of an oxygen atom with hydroxyl group of the surface of perlite, and thus, complexation occurred.[36]

Surface energetics of raw materials and composites

Inverse gas chromatography was applied to check the changes in surface energy as being result of composite manufacturing. Values of the dispersive component of the surface free energy and specific parameters describing the surface's ability to specific interactions are presented in Table 2.

The addition of the filler to the component most often caused the decrease of the dispersive component of surface-free energy. The resulting values were lower than those found for perlit alone. However, this was not the case for the PS-PER composite. The γ_S^d values found for this composite are the highest one – higher than for polymer alone and the filler. It might indicate the more active system when the ability to dispersive interaction is taken into account. Moreover, values of K_A and K_D parameters are also significantly higher for this composite. The tendency of PS-PER composite to act as an electron acceptor is slightly lower than this of PER or PS alone. The ability for electron donor interactions (K_D value) is lower than those of PS while is significantly increased in comparison to the K_D value for PER. However, the surface character of PS-PER remained the same in comparison to the polymer matrix.

TABLE II. Values of dispersive component of the surface free energy (mJ/m^2), K_A, K_D, and S_C of perlite, neat polymers, and perlite/polymer composites

Materials	γ_S^d (mJ/m^2)				K_A	K_D	$S_C=K_D/K_A$
	40ºC	50ºC	60ºC	70ºC			
PER	-	-	34.2	30.9	0.13	0.17	1.3
PVA	41.9	40.9	40.3	39.9	0.06	0.21	3.5
PVA-PER	32.4	30.2	27.9	25.8	0.07	0.14	2.0
PVP	35.4	33.4	31.5	29.7	0.06	0.35	5.8
PVP-PER	24.5	23.9	22.1	21.1	0.06	0.29	4.8
PMMA	40.9	38.2	35.8	33.5	-	-	-
PMMA-PER	32.3	28.9	25.9	23.1	-	-	-
PS	33.7	30.8	27.8	25.1	0.13	0.53	4.0
PS-PER	39.9	37.7	36.7	35.6	0.11	0.41	3.8

Retention data collected during IGC experiments allowed to calculate also values of dispersive (W_a^d), specific (W_a^{sp}) component of work of adhesion between polymer and filler as well as total value of work of adhesion (W_a^{tot}). These parameters might be successfully used as a measure of the magnitude of adhesion between components in complex systems, e.g. composites.[6,7] Values of work of adhesion were determined at different temperatures due to technical problems during examination of e.g. PER in the whole range of temperatures.

TABLE III. Values of dispersive, specific component of the work of adhesion and its total value (mJ/m^2) perlite/polymer composites

Materials	W_a^d (mJ/m^2)				W_a^{sp} (mJ/m^2)		W_a^{tot} (mJ/m^2)	
	40ºC	50ºC	60ºC	70ºC	60ºC	70ºC	60ºC	70ºC
PVA-PER	32.4	30.2	27.9	25.8	29.4	30.6	96.5	94.8
PVP-PER	24.5	23.9	22.1	21.1	27.3	30.3	80.0	80.4
PMMA-PER	32.3	28.9	25.9	23.1	-	-	60.9	55.6
PS-PER	39.9	37.7	36.7	35.6	31.6	32.5	95.5	92.3

Morphological characterization

The microstructure of the perlite was investigated by field emission scanning electron microscopy (Fig. 4). FE-SEM (scale bars 50 and 2 μm) images shows that the perlite particles have an irregular glassy flake shape.

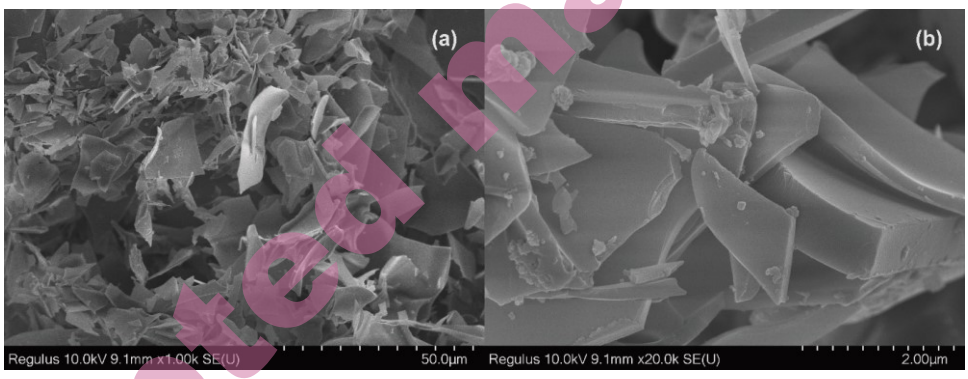

Fig. 4. FE-SEM images of perlite (a) at 1000x magnification, (b) at 2000x magnification.

Figure 5 shows the FE-SEM images of cryo-milled polymer composites. Cryo-milling works with liquid nitrogen medium below the ductile-brittle transition temperature of the polymers. Thus, the polymer is in a fragile state and grinding could be achieved in much shorter times without deformation compared to conventional mechanical milling techniques.[37] It can be observed that there are many fragments of perlite in the whole surface of the PVA matrix (Fig. 5a and 5b), however comparing PVA-PER (Fig. 5a) to other composites (Fig. 5c, 5e ang 5g), it seemed that interfacial adhesion between the perlite and PVA matrix was poor. Fillers are pulled out of the PVA matrix during the cryo-milling. PVP-PER has a smooth fractured surface, typical of a brittle material, other composites have a rougher surface than PVP-PER.

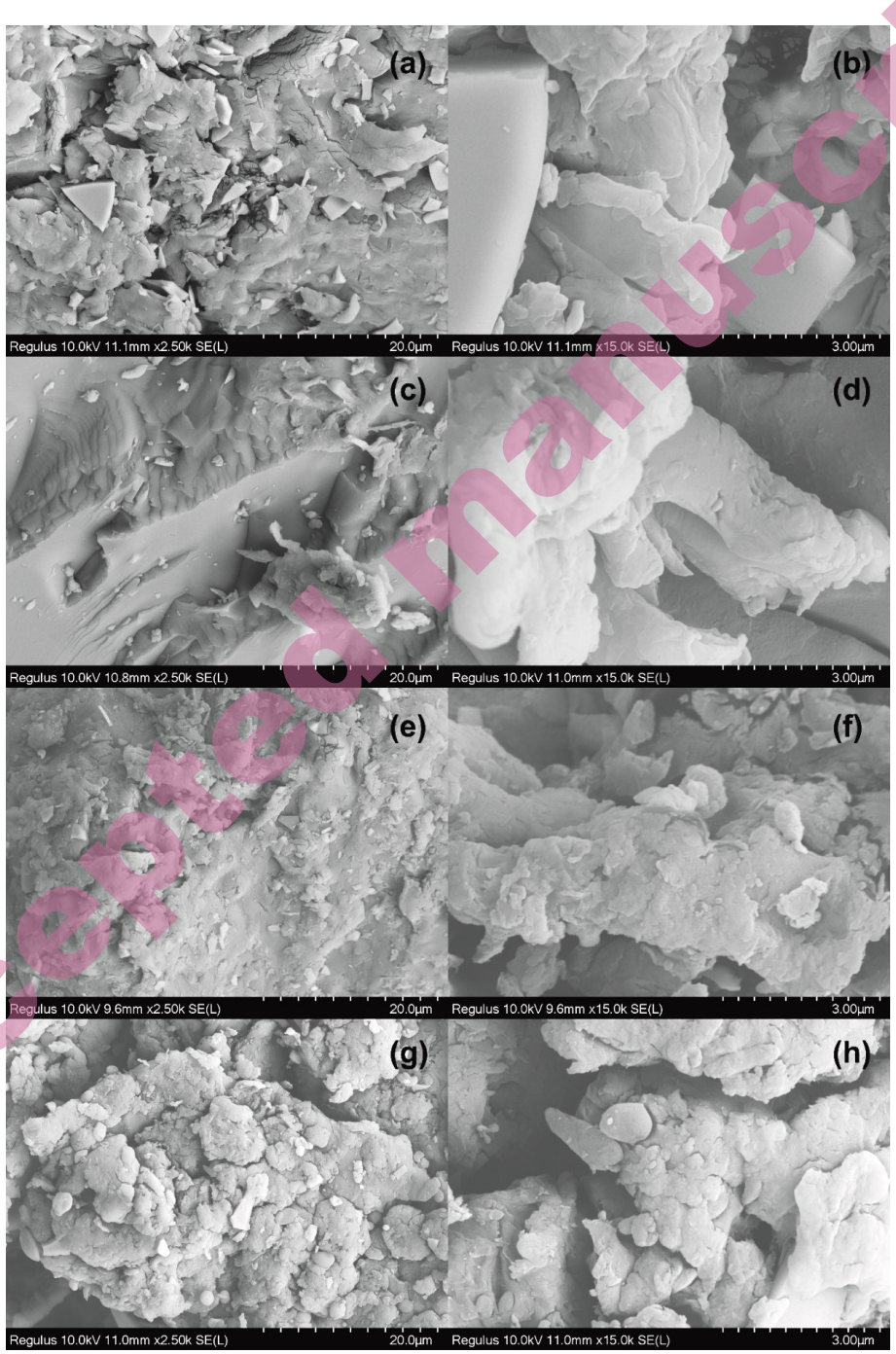

Fig. 5. FE-SEM images of PVA-PER (a and b), PVP-PER (c and d), PMMA-PER (e and f) and PS-PER (g and h).

As can be seen in Fig 5g and 5h, incorporation of perlite results in a more layered structure of the PS matrix, which indicates a strong interaction between the filler and the polymer matrix.[38] This observation is confirmed by high values of work of adhesion between the components of this composite (Table 3). It should be noted that these strong interactions between are attributed to specific interactions. Dispersive component of the work of adhesion is highest for PVA-PER system but it, as shown above, does not assure the stability of composite. However, higher values of W_a^{sp} found for PS-PER composite results in higher stability of the system although total work of adhesion W_a^{tot} is on similar level for these two systems.

TEM analysis was used for the examination of the dispersion of perlite in the polymers (Fig. 6). The examination of the below figures shows that there are no perlite agglomerates in the examined composites.

The intensities of the diffraction peaks of PVA-PER were slightly decreased compared to pure PVA. This was also seen in PVP-PER and PMMA-PER. However, the peak intensities of the PS-PER have been considerably decreased upon the addition of perlite. This change in diffraction intensity can be attributed to the amorphous nature increasing with the perlite incorporation into the polymer.

Within the experimental temperature range, PVA-PER, PVP-PER, and PMMA-PER samples display similar degradation profiles when compared with their corresponding pure polymer matrixes. This means that perlite did not significantly alter the degradation mechanism of PVA, PVP, and PMMA in these conditions. As seen in Fig. 2, the best thermal result was obtained from PS-PER. From Table 1, the $T_{0.5}$ value of pure PS is 412 °C, while that of PS-PER is 438 °C. PS and PS-PER shared a one-step thermal degradation process and the addition of perlite has shifted the decomposition curve of TGA to considerably higher temperature. This can be attributed to the good distribution of the perlite in the PS matrix.

Among all the studied polymers, the most significant change in the FTIR spectrum was seen in PS samples. According to the patterns, the intensity was changed by the incorporation of perlite in the case of PS composite due to the uniform distribution of perlite in the PS matrix[39]. The IR spectra of the PS-PER and PMMA-PER exhibit a band at around 1070 cm^{-1}, corresponding to the asymmetric stretching vibrations of Si–O bonds in perlite.

The dispersive component of the work of adhesion decreases with the increase of the temperature of the IGC experiment. The highest values were found for PVA–PER and PS-PER systems while the lowest for the PVP-PER composite.

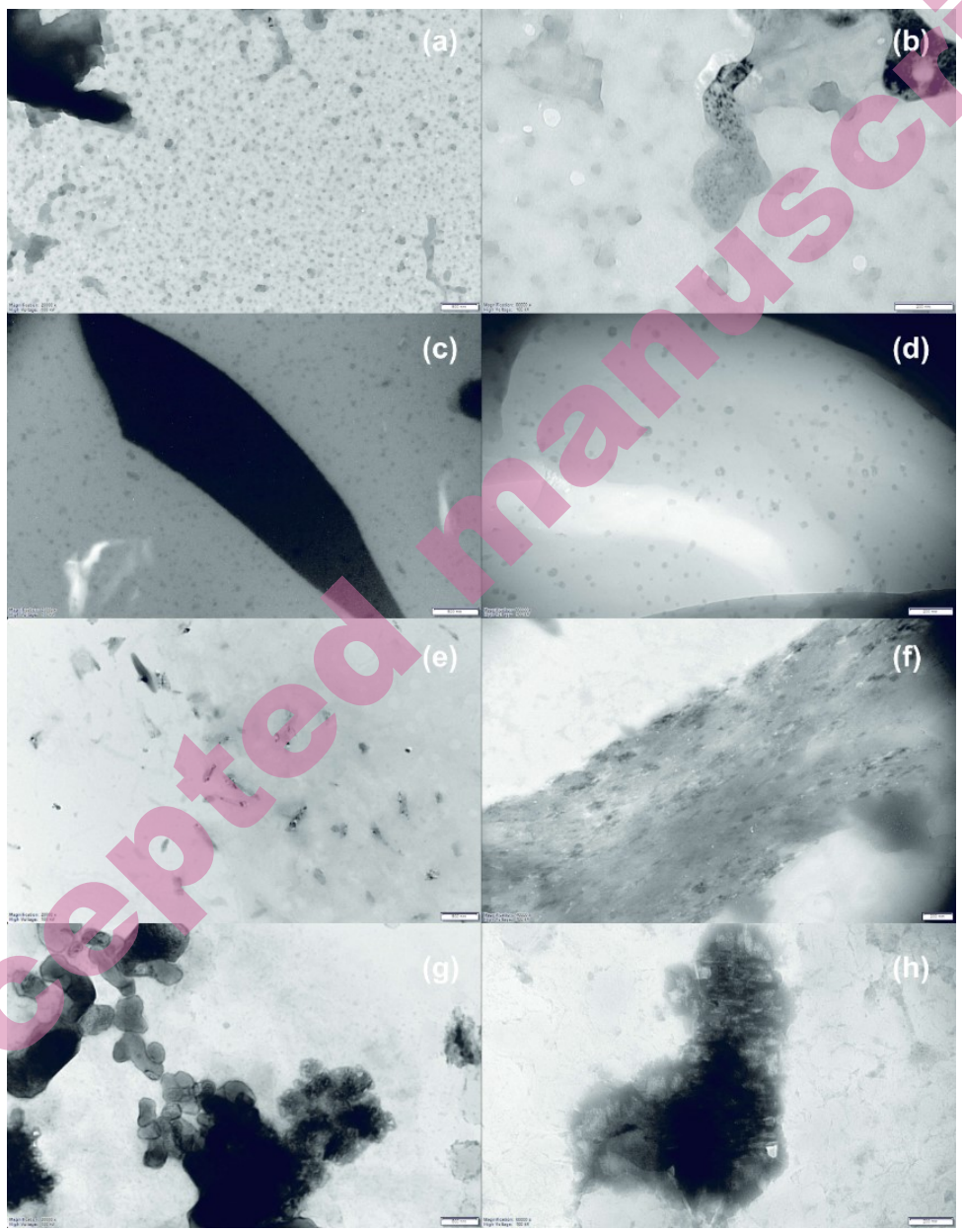

Fig. 6. TEM images for neat PVA-PER (a and b), PVP-PER (c and d), PMMA-PER (e and f), and PS-PER (g and h). Scale bars represent 500 nm (a, c, e and g) and 200 nm (b, d, f and h).

CONCLUSIONS

Perlite is a filler with unique properties, such as low density and thermal conductivity, thus the development of PS/Perlite composites may be interesting for producing lighter packaging with thermal insulation capability.[2] Incorporation of perlite results in a more layered structure of the PS matrix, which indicates a strong interaction between the filler and the polymer matrix. This observation is confirmed by high values of work of adhesion between the components of this composite. It should be noted that these strong interactions are attributed to specific interactions.

1. The distribution of perlite particles in polymer matrix is very important because the distribution of the filler (additive) has a significant effect on the final morphology and properties of polymer nanocomposites. It was determined by XRD analysis whether perlite was distributed homogeneously in the prepared nanocomposites. In general, the formation of intercalated nanocomposites causes an increase in the basal space in the XRD pattern, while the formation of exfoliated nanocomposites causes the patterns between the layers to completely disappear and therefore distinct peaks cannot be observed. In this study, no significant change was observed in the diffraction peaks of the XRD patterns of the nanocomposites prepared using 5 wt% perlite. This result indicates that the perlite particles are brought together by providing a homogeneous distribution in the polymeric matrixes. The compatibility of this situation with many other studies has been confirmed by comparing with the XRD patterns available in the literature.
2. TEM and SEM images, which are complementary to XRD characterizations, are the most popular techniques used to determine the morphology of nanocomposites. In general, the microstructure features obtained from TEM, provide useful details to the overall picture that can be derived from XRD results and support the understanding of various issues involving nanocomposite formation. The distribution microstructure of intercalated and exfoliated perlite layers in this study was also investigated by SEM and TEM analyses. The homogeneous distribution of perlite in the obtained polymer matrix nanocomposites was confirmed by TEM analyses in addition to XRD characterizations. TEM images show that the perlite layers are well-structured and homogeneously distributed within the polymer matrices.
3. The morphologies of nanocomposites are evaluated using SEM and TEM analysis techniques. SEM images provide information about the reinforcement (filler) materials in the composites, dispersion defects and phase boundaries during bonding, surface roughness and cracked surfaces. In this study, SEM analysis was performed to view the surface of the materials and the distribution of the filler (reinforcement) in the polymer matrix. It was observed from the

SEM images that the prepared nanocomposites exhibited a very good distribution.

4. FTIR spectrum of all samples were taken in order to determine structural characterization. As seen from the FTIR spectrum of the obtained nanocomposite, there is not much difference between the spectrum of the neat polymers. This situation supports the formation of homogeneously distributed nanocomposites as a complement to XRD, SEM, TEM characterizations.
5. TGA analyses were performed to determine the thermal characterizations of all samples. It was observed that perlite clay used as filler had high thermal stability. The combustion resistance of polymers is quite low, therefore the use of silicate particles as filler increases their thermal resistance. The thermal resistances of all nanocomposites obtained in this study increased slightly. However, the highest thermal resistance was observed for the PS-PER nanocomposite, and this was achieved as a result of the TGA decomposition curve being shifted to a significantly higher temperature with the addition of perlite filler.
6. One of the most commonly measured parameters for the description of the energy situation on the surface of a solid is the surface energy. The surface energy can affect, for example, catalytic activity or the strength of particle–particle interaction. Due to the important role of surface energy in physicochemical interactions, surface energy measurement has attracted the attention of material and surface researchers. In this study, the highest surface energy value was obtained for PS-PER nanocomposite (γ_s^d = 35.5 mJ/m^2, at 70ºC). This value is even higher than the value obtained for PS-orgona montmorillonite nanocomposite (γ_s^d = 28.9 mJ/m^2, at 70ºC). This situation is quite positive for perlite filled nanocomposites prepared without using any organo modified filler in this study. Based on the obtained results, the synthesized PS-PER composite shows the best performance and is the most suitable for practical applications.
7. The acid or basic properties of solid surfaces are interesting aspects of surface structure, and important in the fields of ion exchange and heterogeneous catalysis. Acid/base catalyzed reactions belong to the technologically most important classes of heterogeneous catalytic conversions. IGC may provided determination of important parameters, including Lewis acid-base interaction parameters between the matrix and filler of composite materials. Determining the changes in this surface property will make a significant contribution to the development of polymer matrix nanocomposites used in many industrial sectors.

Acknowledgements: This work was partly supported by a grant from Polish Ministry of Science and Education.

ИЗВОД

ТЕРМАЛНЕ, МОРФОЛОШКЕ И ПОВРШИНСКЕ ОСОБИНЕ КОМПОЗИТНИХ МАТЕРИЈАЛА СА ПЕРЛИТНИМ ОЈАЧАЊИМА

CEYDA BİLGİÇ[1], NAİLE KARAKEHYA[2], ADAM VOELKEL[3]

[1]Department of Chemical Engineering, Faculty of Engineering and Architecture, Eskişehir Osmangazi University, Eskişehir, Türkiye, [2]Department of Environmental Protection Technologies, Eskişehir Vocational School, Eskişehir Osmangazi University, Eskişehir, Türkiye, and [3]Poznan University of Technology, Institute of Chemical Technology and Engineering, Poznań, Poland.

Овај рад се бави припремом и карактеризацијом композита перлит/поливинил алкохол, перлит/поливинилпиролидон, перлит/полиметил метакрилат и перлит/полистирол. Полимерни композити су припремљени техником ливења раствора са 5 тежинских % перлита као пунила. Перлит је пунило са јединственим особинама, као што су ниска густина и топлотна проводљивост, па развој полимер-перлит композита може бити интересантан за производњу лакше амбалаже са способношћу топлотне изолације. Перлит/полимер нанокомпозити су карактерисани помоћу рендгенске дифракционе (XRD) анализе, термогравиметријске анализе (TGA), Фуријеове трансформационе инфрацрвене спектроскопије (FTIR), инверзне гасне хроматографије (IGC), скенирајуће електронске микроскопије (FE-SEM) и трансмисионе електронске микроскопије (TEM). Мерења TGA су показала значајно повећање термалне стабилности полистирола услед присуства перлита у односу на матрицу. FE-SEM слика криомлевеног узорка показује да су перлитне честице уграђене унутар полистиролне матрице, што је у складу са подацима о адхезији добијеним методом IGC.

(Примљено 8. августа; ревидирано 5. октобра; прихваћено 9. новембра 2024.)

REFERENCES

1. R. Sahraeian, M. Esfandeh, *Polymer Bull.* **74** (2017) 1327 (https://doi.org/10.1007/s00289-016-1779-z)
2. A. G. de Oliveira, J. C. Jandorno, E. B. D. da Rocha, A. M. F. de Sousa, A. L. N. da Silva, *Appl. Clay Sci.* **181** (2019) 105223 (https://doi.org/10.1016/j.clay.2019.105223)
3. M. Doğan, H. Yüksel, B. K. Kizilduman, *Int. J. Mat. Res.* **112** (2021) 405 (https://doi.org/10.1515/ijmr-2020-8007)
4. H. Tian, H. Tagaya, *J. Mat. Sci.* **43** (2008) 766 (https://doi.org/10.1007/s10853-007-2127-3)
5. M. Raji, S. Nekhlaoui, I.-E. El Hassani, E. Essassi, H. Essabir, D. Rodrigue, R. Bouhfid, A. Qaiss, *Composites Part B: Eng*> **165** (2019) 47 (https://doi.org/10.1016/j.compositesb.2018.11.098)
6. B. Strzemiecka, A. Voelkel, *Int. J. Adh. Adhes.* **38** (2012) 84 (https://doi.org/10.1016/j.ijadhadh.2012.05.006)
7. B. Strzemiecka, A. Voelkel, J. Donate-Robles, J. M. Martín-Martínez, *J. Chrom. A* **1314** (2013) 249 (https://doi.org/10.1016/j.chroma.2013.09.040)
8. C. Bilgiç, N. Karakehya, *J. Adh. Sci. Technol.* **30** (2016) 1945 (https://doi.org/10.1080/01694243.2016.1161968)
9. N. Karakehya, *Int. J. Adh. Adhes.* **110** (2021) 102949 (https://doi.org/10.1016/j.ijadhadh.2021.102949)

10. F. Cakar, *Surf. Interf. Anal.* **53** (2021) 258 (https://doi.org/10.1002/sia.6911)
11. A. Voelkel, B. Strzemiecka, K. Adamska, K. Milczewska, *J. Chrom. A* **1216** (2009) 1551 (https://doi.org/10.1016/j.chroma.2008.10.096)
12. A. Voelkel, *Chapter 22 - Physicochemical measurements (inverse gas chromatography)*, in *Handbooks in Separation Science, Gas Chromatography (Second Edition)*, C. F. Poole, Elsevier, Amsterdam, Netherlands, 2021, p. 561. (https://doi.org/10.1016/B978-0-12-820675-1.00013-7)
13. F. Thielmann, *J. Chrom. A* **1037** (2004) 115 (https://doi.org/10.1016/j.chroma.2004.03.060)
14. M. Teodorescu, M. Bercea, S. Morariu, *Biotech. Adv/* **37** (2019) 109 (https://doi.org/10.1016/j.biotechadv.2018.11.008)
15. M. M. Chehimi, M.-L. Abel, C. Perruchot, M. Delamar, S. F. Lascelles, S. P. Armes, *Synth. Metals* **104** (1999) 51 (https://doi.org/10.1016/S0379-6779(99)00040-5)
16. T. Hamieh, M.-B. Fadlallah, J. Schultz, *J. Chrom. A* **969** (2002) 37 (https://doi.org/10.1016/S0021-9673(02)00369-2)
17. A. Aşkın, D. T. Yazıcı, *Chromatographia* **61** (2005) 625 (https://doi.org/10.1365/s10337-005-0558-z)
18. L. Lavielle, J. Schultz, *Langmuir* **7.5** (1991) 978 (https://doi.org/10.1021/la00053a027)
19. B. Lindsay, M.-L. Abel, J. F. Watts, *Carbon* **45.12** (2007) 2433-2444. (https://doi.org/10.1016/j.carbon.2007.04.017)
20. F. Bauer, R. Meyer, M. Bertmer, S. Naumov, M. Al-Naji, J. Wissel, M. Steinhart, D. Enke, *Colloids Surf. A: Physicochem. Eng. Aspects* **618** (2021) 126472 (https://doi.org/10.1016/j.colsurfa.2021.126472)
21. V. Gutmann, *Coord. Chem. Rev.* **2** (1967) 239 (https://doi.org/10.1016/S0010-8545(00)80206-4)
22. F. L. Riddle, F. M. Fowkes, *JACS* **112** (1990) 3259 (https://doi.org/10.1021/ja00165a001)
23. C. J. van Oss, *Interfacial forces in aqueous media*, Taylor & Francis Group, Boca Raton, USA, 2006 (https://doi.org/10.1201/9781420015768)
24. S. S. Uluatam, *J. Amer. Water Works Assoc.* **83** (1991) 70 (https://doi.org/10.1002/j.1551-8833.1991.tb07165.x)
25. E. Kolvari, N. Koukabi, M. M. Hosseini, *J. Mol. Cat. A: Chem.* **397** (2015) 68 (https://doi.org/10.1016/j.molcata.2014.10.026)
26. L. A. García-Cerda, M. U. Escareño-Castro, M. Salazar-Zertuche, *J. Non-Cryst. Solids* **353** (2007) 808 (https://doi.org/10.1016/j.jnoncrysol.2006.12.046)
27. Y.-H. Wu, D.-G. Yu, H.-P. Li, X.-Y. Wu, X.-Y. Li, *e-Polymers* **17.1** (2017) 39 (https://doi.org/10.1515/epoly-2016-0244)
28. I. S. Tsagkalias, T. K. Manios, D. S. Achilias, *Polymers* **9** (2017) 432 (https://doi.org/10.3390/polym9090432)
29. T. E. Motaung, A. S. Luyt, M. L. Saladino, D. C. Martino, E. Caponetti, *Exp. Polymer Lett.* **6** (2012) 871 (https://doi.org/10.3144/expresspolymlett.2012.93)
30. A. M. Hussein, E. M. A. Dannoun, S. B. Aziz, M. A. Brza, R. T. Abdulwahid, S. A. Hussen, S. Rostam, D. M. T. Mustafa, D. S. Muhammad, *Polymers* **12** (2020) 2320 (https://doi.org/10.3390/polym12102320)
31. N.A. Betti, *Eng. Technol. J. Part A* **34** (2016) 2433 (https://doi.org/10.30684/etj.34.13A.6)

32. L. Moradi, M. Mirzaei, *RSC Adv.* **9** (2019) 19940 (https://doi.org/10.1039/C9RA03312B)
33. K. Srivastava, N. Shringi, V. Devra, A. Rani, *Int. J. Innov. Res. Sci. Eng. Techn.* **2** (2013) 2936 (https://www.ijirset.com/upload/july/49_%20Pure%20Silica.pdf)
34. Z. Zujovic, W. V. K. Wheelwright, P. A. Kilmartin, J. V. Hanna, R. P. Cooney, *Ceramics Int.* **44** (2018) 2952 (https://doi.org/10.1016/j.ceramint.2017.11.047)
35. P. Spasojević, V. Panić, S. Šešlija, V. Nikolić, I. Popović, S. Veličković, *J. Serb. Chem. Soc.* **80** (2015) 1177 (https://doi.org/10.2298/JSC150123034S)
36. S. Ramesh, L. C. Wen, *Ionics* **16** (2010) 255 (https://doi.org/10.1007/s11581-009-0388-3)
37. M. Robotti, S. Dosta, I. G. Cano, A. Concustell, N. Cinca, J. M. Guilemany, *Adv. Pow. Techn.* **27** (2016) 1257 (https://doi.org/10.1016/j.apt.2016.04.014)
38. M. Nisar, M. da Graça Sebag Bernd, C. P. da Silva Filho Luiz, J. Geshev, N. R. de Souza Basso, G. B. Galland, *J. App. Pol. Sci.* **135** (2018) 46820. (https://doi.org/10.1002/app.46820)
39. A. Mostafaei, A. Zolriasatein, *Prog. Nat. Sci.: Mat. Int.* **22** (2012) 273 (https://doi.org/10.1016/j.pnsc.2012.07.002).